PCCP

Accepted Manuscript

ROYAL SOCIETY OF CHEMISTRY

www.rsc.org/pccp

PCCP

ARTICLE

The origin of a large apparent tortuosity factor for the Knudsen diffusion inside monoliths of a samaria-alumina aerogel catalyst: a diffusion NMR study

Received 00th January 20xx,
Accepted 00th January 20xx

DOI: 10.1039/x0xx00000x

www.rsc.org/

R. Mueller,[a] S. Zhang,[a] M. Klink,[b] M. Bäumer*[b] and S. Vasenkov*[a]

Pulsed field gradient (PFG) NMR was applied to measure tortuosity factors for carbon dioxide diffusion in the Knudsen and gas regimes inside monoliths of a samaria-alumina aerogel catalyst, a high porosity material containing micropores in addition to meso- and macropores. The apparent tortuosity factor obtained from PFG NMR measurements for the Knudsen diffusion in the meso- and macropores of the catalyst has an unexpectedly large value of approximately 6 if carbon dioxide adsorption in the micropores and other types of surface adsorption sites of the catalyst is ignored. At the same time, the corresponding apparent tortuosity factor in the gas regime was found to be around 2. Application of a proposed model which describes fast molecular exchange between the surface adsorption sites and the main pore volume of the catalyst yields corrected tortuosity factors which depend only on the pore system geometry. Using this model, the corrected tortuosity factors were found to be around 2 for both diffusion regimes, in agreement with the expectations based on a high porosity of the studied catalyst.

Introduction

Recent progress in sol-gel synthesis has resulted in the development of relatively simple and inexpensive experimental procedures suitable for forming aerogel catalysts.[1-11] These materials usually exhibit large porosity (≥ 0.95) and a broad distribution over pore sizes where the majority of pores fall in the mesopore and macropore ranges. Active sites are located on pore walls of aerogel catalysts. Hence, these sites are directly accessible for guest molecules. Among several types of aerogel catalysts, rare-earth aerogels are of significant interest for catalytic reaction involving light gases.[8-11] In particular, samaria and samaria-alumina aerogels represent promising catalysts for the oxidative coupling of methane (OCM).[12, 13] It is important to note that samarium can be used as a structure promotor to increase the stability of alumina and other catalyst supports developed for gas phase reactions including CO_2 methanation and methane steam reforming.[14, 15]

The transport of reactant and product molecules inside meso- and macropores of catalysts can play a large role in the catalytic performance. The transport properties of such catalysts can be characterized by the tortuosity factor (η), which provides a means of quantifying the extent of increased molecular trajectories in porous systems due to multiple reflections from the porous structure. A known value of molecular self-diffusivity (D) in the pore systems of catalysts can be used to calculate the tortuosity factor[16, 17]

$$\eta = D_0 / D, \qquad (1)$$

where D_0 is the corresponding reference self-diffusivity. Two reference diffusivities can be defined for the diffusion of gases, one for the Knudsen regime when molecule-solid collisions occur much more frequently than molecule-molecule collisions and another for the gas diffusion regime when molecule-molecule collisions dominate. The reference diffusivity in the Knudsen regime (D_{K0}) is usually assumed to be equal to that for the diffusion of gas molecules confined within straight parallel cylindrical pores with the diameter equal to the mean intercept length (d) in the considered pore system

$$D_{K0} = \frac{1}{3}\bar{u}d, \qquad (2)$$

where $\bar{u} = (8RT/\pi M)^{0.5}$ is the mean thermal velocity at temperature T, R is the gas constant and M is the molar mass. The reference diffusivity in the gas diffusion regime (D_{g0}) can be defined as the diffusivity in the macroscopic gas volume surrounding the

a. Department of Chemical Engineering, University of Florida, Gainesville, FL 32611, United States
b. Institute for Applied and Physical Chemistry, University of Bremen, 28359, Bremen, Germany
* M. Bäumer, Phone: +49 421 218 63171. Fax: +49 421 218 63188. E-mail: mbaeumer@uni-bremen.de.
*S. Vasenkov. Phone: +1 352 392 0315. Fax: +1 352 392 0315. E-mail: svasenkov@che.ufl.edu.
Electronic Supplementary Information (ESI) available: Results of least-squares fitting of the diffusion data

porous material under the equilibrium conditions. The tortuosity factors in the two regimes are given by

$$\eta_K = D_{K0}/D_K, \qquad \eta_g = D_{g0}/D_g, \tag{3}$$

where D_K and D_g are, respectively, the self-diffusivities in the Knudsen and gas regime in the considered porous system. In the general case when both molecule-molecule and molecule-solid collisions contribute to the diffusion process the overall self-diffusivity in the pores ($D_{p\ model}$) can be estimated using the Bosanquet-type approximation[18]

$$\frac{1}{D_{\mathrm{p\,model}}} = \frac{1}{D_K} + \frac{1}{D_g} = \frac{\eta_K}{D_{K0}} + \frac{\eta_g}{D_{g0}}, \tag{4}$$

where the expression in the right-hand part of Eq. 4 was obtained using Eq. 3. Kinetic Monte Carlo (KMC) simulations of gas diffusion in porous systems revealed that η_K can be much larger than η_g due to deviations of the molecular trajectories in the Knudsen regime from those which are usually assumed based on the analogy with the diffusion in the gas regime.[18-20] In particular, these deviations can arise as a result of correlations between the directions of trajectory segments in the Knudsen regime.[20] Tortuosity factors that are larger in the Knudsen regime than in the gas regime were also observed experimentally for diffusion in zeolite beds.[21] In all these cases when $\eta_K > \eta_g$ the system porosity was usually much smaller than 1 and the tortuosity factor in the Knudsen regime was larger than 2. In high porosity systems like aerogel catalysts, Knudsen regime tortuosity factors around 2 or smaller are predicted by models based on the Maxwell equation and other approaches that relate tortuosity and porosity.[22, 23]

In this work ^{13}C PFG NMR was used to measure tortuosity factors for diffusion of CO_2 molecules inside macroscopic particles (i.e. monoliths) of samaria-alumina aerogel catalyst. CO_2 was chosen as a representative probe molecule because it is one of the reactants or products in many gas-phase reactions of interest for samaria-alumina aerogel catalysts.[12-15] Owing to a very broad range of CO_2 densities used in the PFG NMR diffusion studies it was possible to obtain tortuosity factors for both the Knudsen and gas regimes of diffusion inside the catalyst monoliths. Applying Eq. 4 to the measured CO_2 self-diffusivity in the samaria-alumina aerogel catalyst the apparent tortuosity factor in the Knudsen regime was found to be around 6.4, which is more than a factor of 3 larger than that in the gas regime. A model explaining the origin of the large value of the tortuosity factor in the Knudsen regime and the large difference in the apparent tortuosity factors in the two regimes is presented and discussed. It will be demonstrated that using the reported NMR data it is possible to calculate the corrected tortuosity factors that depend only on the topological properties of the catalyst. The corrected tortuosity factors were found to be similar for the Knudsen and gas regimes. Their values (~ 2) are in agreement with the expectations based on the large porosity of the studied catalyst.[22, 23] The corrected tortuosity factors were found to be comparable with the tortuosity factor in the gas regime (~1.7) observed for diffusion in the gaps between microscopic particles of the aerogel catalyst in a particle bed.[24]

Experimental

A sample of alumina stabilized samaria-alumina aerogel was formed using the sol-gel method presented in Refs.25, 26. A sol was prepared by dissolving a mixture of 95 mol % of aluminum chloride hexahydrate (Alfa) and 5 mol % of samarium (III) chloride hexahydrate (Chempur, Karlsruhe, Germany) in an absolute ethanol (Roth, Germany) and water solution prepared at around 20:1 volume ratio. Propylene oxide (Sigma Aldrich) was used as the gelation agent. The sols were sealed inside cylindrical PTFE vials (6 mm diameter) and allowed to gel and age for at least 24 hours under ambient conditions. The resulting gels were then immersed in a bath of absolute ethanol where they were washed three times in three days, changing the ethanol daily. These alcogels were processed to aerogels in a BALTEC supercritical point drier. The alcohol in the gel pores was exchanged for liquid CO_2 for 3 days at about 285 K, after which the temperature of the vessel was ramped up to about 318 K while not exceeding a pressure of around 10^4 kPa. The vessel was then depressurized at a rate of about 700 kPa per hour. The formed aerogel monoliths were calcined at 973 K. The monoliths have a shape of a cylinder with a diameter of about 2-3 mm and a length of around 10-20 mm. The density of an aerogel monolith was found to be approximately 0.21 g/cm^3.

Nitrogen adsorption isotherms were measured at 77 K using a QuadraSorb sorption analyzer (Quantachrome Instrument Corp.) after degassing the aerogel sample for 120 hours at 523 K. Density functional theory (DFT) and the Barrett-Joyner-Halenda (BJH) method were used, respectively, for obtaining the pore size distributions in the micro-/mesopore and meso-/macropore ranges from the measured N_2 adsorption isotherms. Based on the N_2 adsorption isotherm data and the known volume of the catalyst monoliths used in the measurements the particle porosity is estimated to be 0.96±0.03. This value is in agreement with the expectations for aerogels.

To prepare a sample for PFG NMR studies, one or two aerogel monoliths were placed into a 5 mm NMR tube. For sample activation (i.e. degassing) and loading with CO_2 the NMR tube with the sample was connected to a custom-made vacuum system. The activation was performed under high vacuum (< 10^{-3} Pa) at 473 K for at least 24 hours. Activated sample was loaded with CO_2 (Sigma-Aldrich, 99% ^{13}C isotopic enrichment) by either exposing it to the gas at the desired pressure for at least 4 hours at 298 K or by cryogenically freezing the desired quantity of CO_2 from a calibrated volume of the vacuum system using liquid nitrogen. After loading with CO_2, the NMR tube with the sample was flame sealed and separated from the vacuum system. PFG NMR diffusion measurements were performed using a 17.6 T Bruker BioSpin NMR

spectrometer operating at ^{13}C resonance frequency of 188.6 MHz. Sine-shaped magnetic field gradients with the effective duration of 120-200 µs and amplitude up to 3 T/m were generated using diff60 diffusion probe (Bruker BioSpin) and Great60 gradient amplifier (Bruker BioSpin). The standard PFG NMR stimulated echo pulse sequence with longitudinal eddy current delay (PGSTE LED) was used.[27] This sequence can be schematically presented as $\pi/2$-τ_1-$\pi/2$-τ_2-$\pi/2$-τ_1-$\pi/2$-τ_e-$\pi/2$-echo where the gradient pulses are applied during the time intervals τ_1. The absence of disturbing magnetic susceptibility effects was confirmed by verifying that the diffusion data obtained for different values of τ_1 in the range between 0.4 and 1.5 ms were the same within the experimental uncertainty.[28] The longitudinal eddy current delay τ_e was between 0 and 1.5 ms.

Self-diffusivities were obtained from ^{13}C PFG NMR attenuation curves, viz. the dependences of the normalized PFG NMR signal intensity (S) on the amplitude of the magnetic field gradient (g). For the considered case of CO_2 diffusion S was equal to the area under the single ^{13}C NMR line of CO_2. For normal diffusion the signal attenuation (Ψ) is given by the following relation[17, 29]

$$\Psi \equiv \frac{S(g)}{S(g \approx 0)} = \exp(-Dq^2 t), \quad (5)$$

where t is the time of observation of diffusion process (i.e. diffusion time) and q is defined to be $\gamma g \delta$ where γ is the gyromagnetic ratio, δ is the effective gradient pulse length. In the case of normal self-diffusion in three dimensions, the mean square displacement (MSD) can be obtained using the Einstein relation

$$< r^2(t) >= 6Dt. \quad (6)$$

Longitudinal (T_1) and transverse (T_2) ^{13}C NMR relaxation times of CO_2 inside the catalyst monoliths were measured using the inversion-recovery and Carr-Purcell-Meiboom-Gill pulse sequences, respectively.[29] Under our experimental conditions the T_1 relaxation time varied between about 30 ms at an equilibrium sorbate loading pressure of 10 kPa and 250 ms at 10^3 kPa. At the same time, the T_2 relaxation time varied between about 2 ms at a loading pressure of 10 kPa and about 70 ms at 10^3 kPa. The T_1 and T_2 NMR relaxation curves were consistent with only one relaxation ensemble at each loading pressure. All NMR measurements were performed at 297 K.

Results and discussion

Fig. 1 shows the pore size distribution resulting from the measurements of the N_2 adsorption isotherms. The values on the vertical scales in the figure are relative pore volumes divided by the interval of pore sizes between two adjacent points obtained by the same method. This interval was chosen to be much smaller for the DFT method than for the BJH method, resulting in the differences of the value ranges on the vertical scales for the two methods. The average pore size given by the first moment of the pore size distribution was found to be around 75 nm. Fig. 2 shows examples of ^{13}C PFG NMR attenuation curves for CO_2 diffusion inside the catalyst monoliths at different diffusion times and different equilibrium CO_2 pressures in the gas phase surrounding the monoliths. These attenuation curves do not have any contributions from CO_2 molecules that diffuse only in the gas phase of the samples over the duration of diffusion time.

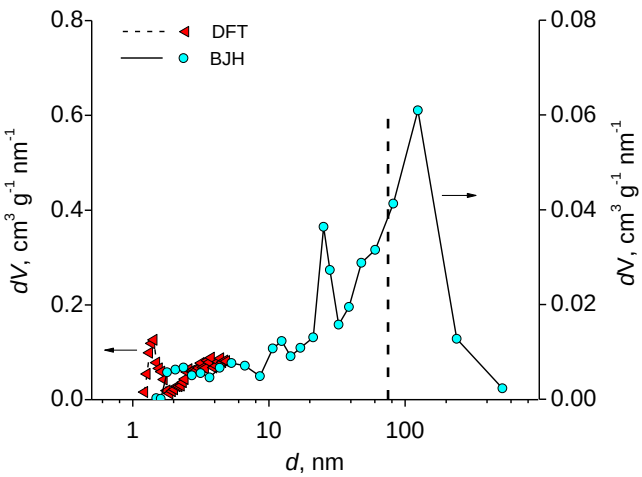

Figure 1. Pore size distributions of the studied samaria-alumina aerogel catalyst. The distributions were obtained from the N_2 adsorption isotherms by applying density functional theory (triangles, left-axis) and Barrett-Joyner-Halenda method (circles, right-axis). The pore size distributions have been scaled such that the areas under the distributions are proportional to the calculated total volume by the corresponding adsorption model. The line segments connecting the points serve as a guide to the eye. The vertical dashed line shows the first moment of the pore size distribution.

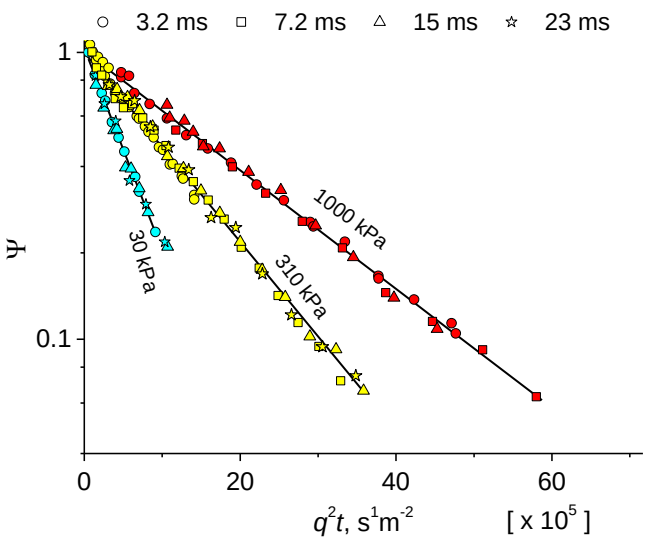

Figure 2. Examples of ^{13}C PFG NMR attenuation curves for CO_2 self-diffusion inside the aerogel catalyst for several diffusion times and CO_2 loading pressures at 297 K. In this presentation, the contribution of the gas phase surrounding the catalyst monoliths have been subtracted away revealing only intraparticle diffusion attenuation.

Such contributions have been subtracted away for clarity of the presentation in the same way as discussed in Ref. 30. Fig. 2 shows that in agreement with Eq. 5 the attenuation curves are linear in the semi-logarithmic presentation of the figure. It is also seen that the attenuation curves measured for the same CO_2 pressure and different diffusion times collapse into a single line as prescribed by Eq. 5 for the case of normal diffusion with a single, time-independent diffusivity. These data indicate that for each loading pressure the CO_2 diffusivity is the same everywhere inside the monoliths. Hence, we can conclude that under our measurement conditions the particle transport properties are uniform. The fitting of the attenuation curves in Fig. 2 using Eq. 5 resulted in the intraparticle diffusivities of CO_2 molecules (D_{intra}) that are presented in Fig. 3 and Table S1 (see electronic supplementary information) as a function of the CO_2 pressure in the surrounding gas phase. It was verified that for the measured range of the diffusion times the values of root MSD, which were obtained for diffusion inside the catalyst monoliths using Eq. 6, were much smaller than the smallest dimension of the monoliths (2 mm). Hence, the measured intraparticle diffusivities are not expected to be perturbed by any effects at the particle boundaries. In addition to the intraparticle diffusivities, Fig. 3 also shows the corresponding CO_2 reference diffusivities in the gas and Knudsen regimes. The reference diffusivities in the gas regime (D_{g0}) for all the pressures except for the smallest pressure of 10 kPa were measured by ^{13}C PFG NMR in the NMR tubes that contained only CO_2 gas (no porous material added). The reference diffusivity in the gas regime at the pressure p = 10 kPa could not be measured by PFG NMR because of the insufficient signal-to-noise ratio. This diffusivity was obtained by the extrapolation of the corresponding diffusivities measured at higher pressures using the expected proportionality between D_{g0} and $1/p$.[17] It was verified that the values of D_{g0} in Fig. 3 are in agreement with the corresponding diffusivities calculated using the kinetic theory of gases as discussed in detail in our previous work.[24]

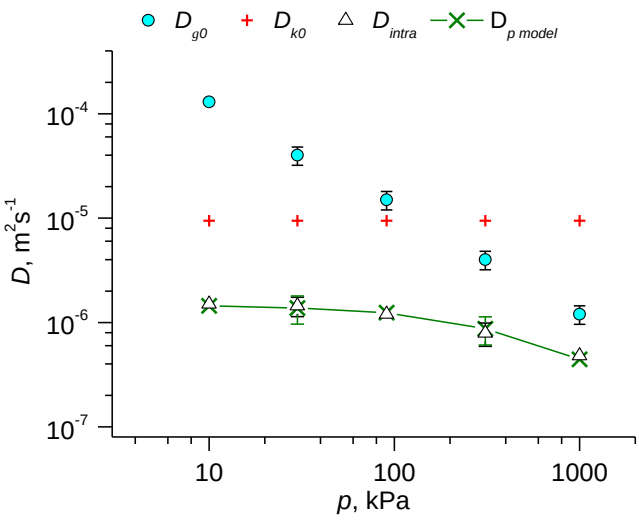

Figure 3. CO_2 self-diffusivity, D_{intra}, measured by ^{13}C PFG NMR inside the monoliths of the studied samaria-alumina aerogel catalyst at 297 K and the corresponding theoretical diffusivity, $D_{p\ model}$, obtained by least-squares regression of the diffusion data shown in the figure to Eq. 4. Also shown are the following self-diffusivities of CO_2 molecules at 297 K: self-diffusivity in the macroscopic gas volume surrounding the catalyst (D_{g0}), and the reference self-diffusivity in the Knudsen regime estimated by using Eq. 2 with d = 75 nm (D_{K0}). All diffusivities are presented as a function of the CO_2 equilibrium pressure in the gas volume surrounding the catalyst monoliths at 297 K.

The reference diffusivity in the Knudsen regime (D_{K0}) was estimated using Eq. 2 where it was assumed that the mean intercept length d is equal to the first moment of the intraparticle pore size distribution (75 nm). It is possible to estimate the tortuosity factors for the diffusion in both regimes inside the particles knowing the values of the intraparticle diffusivities and the corresponding reference diffusivities in the gas and Knudsen regimes for a broad range of CO_2 pressures between 10 and 1000 kPa. The tortuosity factors were obtained by least-squares fitting of the diffusion data in Fig. 3 to Eq. 4, assuming that the measured intraparticle diffusivity (D_{intra}) is equal to $D_{p\ model}$ in Eq. 4. The resulting tortuosity values were found to be equal to 1.9 ± 0.4 and 6.4 ± 1 for the gas and Knudsen regimes, respectively. The best-fit values of the intraparticle diffusivity ($D_{p\ model}$), which were calculated using Eq. 4 with these tortuosity factors, are shown in Fig. 3 and also in Table S1.

Considering the fact that the porosity of the studied aerogel catalyst is around 0.96, the value of 6.4 obtained for the tortuosity factor in the Knudsen regime is surprisingly high. Indeed, the known correlations between the porosity and tortuosity suggest a much lower value of around 2 or smaller for a typical tortuosity factor in such high porosity system.[22,23] The observed large difference between the tortuosity factors in the gas and Knudsen regime is also surprising in view of the large porosity of the studied catalyst. Recent PFG NMR studies of diffusion of organic liquids in mesoporous catalysts have demonstrated that the apparent tortuosity factor obtained from PFG NMR measurements can depend on the reactive chemical functionalities of diffusing molecules.[31,32] The PFG NMR data reported in these papers suggest that the apparent tortuosity factor heavily dependents on the physical and chemical interactions within the porous medium. Clearly, strong molecule-solid interactions can also influence the apparent tortuosity factors measured by PFG NMR in the current study of CO_2 diffusion in the aerogel catalyst. In the case of attractive interactions an increase of the CO_2 density inside the pores relative to the surrounding gas phase is expected. This consideration provides a motivation for comparing the average CO_2 concentration inside the catalyst pores with the CO_2 concentration in the surrounding gas phase.

The CO_2 concentration in the catalyst monoliths was determined by comparing the NMR signal of CO_2 in the catalyst samples with the signal from the NMR tube containing only a known quantity of CO_2 gas in the same way as discussed in Refs. 30, 33. These data and the known catalyst porosity were used to calculate the CO_2 concentration inside the catalyst pores, i.e. the

intrapore concentration. Fig. 4 presents the intrapore concentrations and the corresponding CO_2 concentrations in the surrounding gas phase as a function of the CO_2 pressure in the gas phase at 297 K. The van der Waals equation of state was used to relate pressure and concentration in the gas phase. Fig. 4 shows that at small pressures the intrapore concentration is more than a factor of 3 larger than that in the surrounding gas phase.

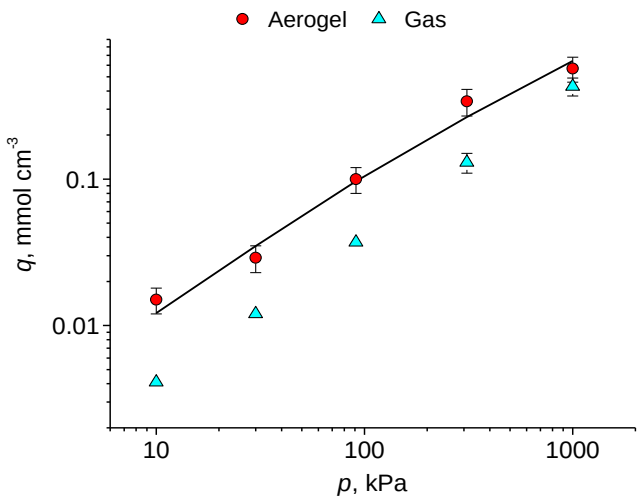

Figure 4. Mean CO_2 density inside the pores of the aerogel catalyst and CO_2 density in the gas phase surrounding the catalyst monoliths as a function of the CO_2 pressure in the gas phase at 297 K. Solid line shows the best fit of the experimental data for the aerogel catalyst to Eq. 7.

This indicates a strong interaction between CO_2 molecules and the pore walls. With increasing CO_2 pressure the difference between the intrapore and gas phase concentrations becomes smaller and, within the experimental uncertainty, disappears at the largest CO_2 pressure (Fig. 4). This behavior is typical for the saturation of a limited number of surface adsorption sites with CO_2 molecules as the molecular density in the pores increases. The role of such adsorption sites can be played by micropores present in the catalyst. In contrast, formation of carbonate and bicarbonate species,[34,35] which is expected for alumina-based materials in the presence of CO_2, is unlikely to contribute to the adsorption process observed by NMR (Fig. 4) because of the low mobility and the resulting dramatic line broadening of the NMR spectrum of such species. Since the length scale of strong interactions between CO_2 molecules and adsorption surface is not expected to be much larger than 1 nm, it can be assumed that the CO_2 density in the main volume of the meso- and macropores of the samaria-alumina aerogel catalyst is the same as in the surrounding gas phase. Based on this expectation, the CO_2 density inside the catalyst pores (q_{ads}) was approximated as a sum of the CO_2 density in the gas phase surrounding the catalyst monoliths (q_{gas}) and an additional density due to adsorption in the surface adsorption sites (q_{surf})

$$q_{ads} = q_{gas} + q_{surf} = q_{gas} + q_{surf\,\max}\frac{bp}{1+bp}, \qquad (7)$$

where the expression in the right-hand part was obtained by using the Langmuir adsorption model for q_{surf}. Least-squares fitting of the data for q_{ads} to Eq. 7 yields satisfactory fit (Fig. 4) with the best fit values of 0.29 mmol cm^{-3} and 0.0029 kPa^{-1}for $q_{surf\ max}$ and b, respectively. The parameter $q_{surf\ max}$ indicates the maximum concentration of CO_2 molecules in the pores due to adsorption in the surface adsorption sites. Assuming that the CO_2 density in the combined volume of these sites at the maximum loading is equal to the density of saturated liquid carbon dioxide at 297 K (~0.8 g cm^{-3}) we estimate that the combined volume of the sites is approximately 1.6×10^{-2}cm^3 per 1 cm^3 of the catalyst pore volume. This combined volume corresponds to around 30% of the total micropore volume (0.24 cm^3/g) determined from the N_2 adsorption isotherm data. Hence, the micropore volume in the catalyst is sufficiently large to assume that the discussed above adsorption in the surface adsorption sites occurs *only* in micropores. In the presence of CO_2, the micropore volume available for CO_2 molecules can be smaller than that obtained from the N_2 adsorption isotherm measurements because of the expected formation of carbonate and bicarbonate species on the micropore walls.[34,35] As discussed above, such species are likely to remain undetectable in the reported NMR measurements and lead to a significant reduction of the micropore volume available for CO_2. Clearly, such micropore volume reduction results in an even better agreement between the available micropore volume and the estimated volume of CO_2 adsorbed in the surface adsorption sites at the maximum density.

Under our experimental conditions we have observed a single self-diffusivity value as well as single values of T_1 and T_2 NMR relaxation times for each CO_2 pressure at 297 K. Hence, it can be assumed that on the time scale of diffusion observation by PFG NMR there is a fast molecular exchange between the surface adsorption sites and the volume of the meso- and macropores for mobile CO_2 molecules that are detected in the NMR diffusion studies. In this case, the diffusivity measured by PFG NMR (D_{intra}) can be approximated as the weighted sum of the surface diffusivity (D_{surf}) and the gas phase diffusivity in the meso- and macropores ($D_{p\ model}$)[17]

$$D_{\text{intra model}} = p_{surf}D_{surf} + (1 - p_{surf})D_{\text{p model}}, \qquad (8)$$

where p_{surf} denotes the fractions of CO_2 molecules in the surface adsorption sites at any given time under the considered steady-state conditions. For any CO_2 pressure, the value of p_{surf} is given by

$$p_{surf} = \frac{q_{surf}}{q_{ads}}. \qquad (9)$$

Substituting the data in Fig. 4 into Eq. 9 allows obtaining the values of p_{surf}, which are found to be in the range between around 0.7 and 0.25 under our experimental conditions. Surface diffusivities are expected to be more than 2 orders of magnitude lower than the

corresponding bulk diffusivities.[17,36,37] Hence, under our experimental conditions the first term in the right-hand part of Eq. 8 can be neglected because it is expected to be much smaller than the second term. As a result, Eq. 8 can be re-written using Eqs. 7 and 9 as follows

$$D_{\text{intra model}} = \frac{q_{gas}}{q_{ads}} D_{\text{p model}} = \frac{q_{gas}}{q_{ads}} \left(\frac{\eta_K}{D_{K0}} + \frac{\eta_g}{D_{g0}} \right)^{-1}, \quad (10)$$

where the expression in the right-hand part was obtained using Eq. 4. Least-squares fitting of the diffusion data in Fig. 3 (which are also shown again in Fig. 5) to Eq. 10 resulted in the tortuosity factors of 1.5 ± 0.3 and 2.0 ± 0.4 for the gas and Knudsen regimes, respectively. These tortuosity factors are in agreement with the expectations based on the high porosity of the studied aerogel catalyst.[22,23] The best-fit values of $D_{intra\ model}$, which were calculated using Eq. 10 with these tortuosity factors, are shown in Fig. 5 and also in Table S2. It is seen that there is a satisfactory agreement between the values of $D_{intra\ model}$ and D_{intra} for each CO_2 pressure used in the measurements. This observation supports the applicability of Eq. 10.

The tortuosity factors obtained by Eq. 10 are similar or, within the experimental uncertainty, even the same in both regimes. It was verified that least squares fitting of the diffusion data in Fig. 4 to an equation, which is a modification of Eq. 10 where η_K and η_g are replaced by η ($\eta_K = \eta_g \equiv \eta$), resulted in a similarly good agreement between the values of $D_{intra\ model}$ and D_{intra} as that in Fig. 5. This agreement is demonstrated in Fig. S1 and Table S3. The tortuosity factor η obtained by the least-squares regression using the modified Eq. 10 with $\eta_K = \eta_g \equiv \eta$ was found to be 1.8 ± 0.4.

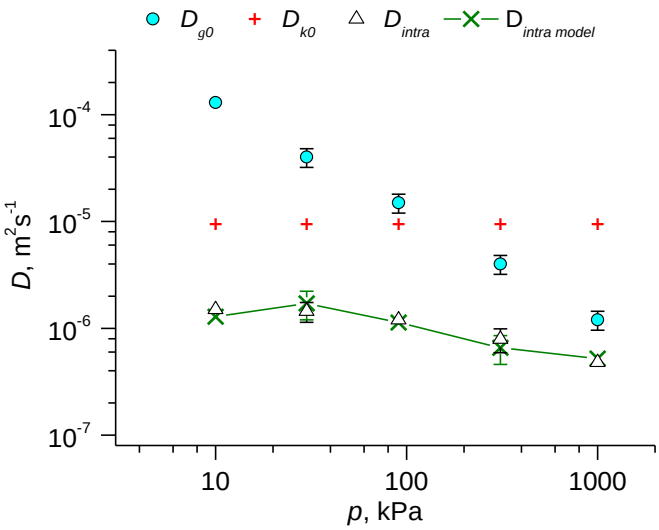

Figure 5. CO_2 self-diffusivity, D_{intra}, measured by ^{13}C PFG NMR inside the monoliths of the studied samaria-alumina aerogel catalyst at 297 K and the corresponding theoretical diffusivity, $D_{intra\ model}$, obtained by least-squares regression of the diffusion data shown in the figure to Eq. 10. Also shown are the following self-diffusivities of CO_2 molecules at 297 K: self-diffusivity in the macroscopic gas volume surrounding the catalyst (D_{g0}), and the reference self-diffusivity in the Knudsen regime estimated by using Eq. 2 with d = 75 nm (D_{K0}). All diffusivities are presented as a function of the CO_2 equilibrium pressure in the gas volume surrounding the catalyst monoliths at 297 K.

Conclusions

Analysis of the ^{13}C PFG NMR data reported in this work for diffusion of CO_2 molecules in the monoliths of the samaria-alumina aerogel catalyst demonstrates that it is possible to separate the contribution from surface diffusion into the apparent tortuosity factor measured for the catalyst using PFG NMR. It is shown that without separating this contribution the apparent tortuosity factor obtained in the Knudsen regime by PFG NMR can be several times larger than the corrected tortuosity, i.e. the traditionally-defined tortuosity which for a given diffusion regime depends only on the geometrical properties of a porous system. Using the reported analysis, the corrected tortuosity factor was found to be around 2 for both the Knudsen and gas regimes in the studied aerogel catalyst. This value is in agreement with the expectations based on the high porosity of the catalyst.

Acknowledgements

We are grateful for the financial support of this work by the NSF CAREER award (CBET No. 0951812). S.V. thanks Hanse-Wissenschaftskolleg (HWK), Germany for the support in the form of a research fellowship. A portion of this work was performed in the McKnight Brain Institute at the National High Magnetic Field Laboratory's AMRIS Facility, which is supported by National Science Foundation Cooperative Agreement No. DMR-1157490 and the State of Florida. Members of the Vasenkov Group would especially like to thank Dan Plant at AMRIS for his help with NMR measurements. We are very grateful to Dr. Björn Neumann for numerous discussions of this work and for preparing the sample of the samaria-alumina aerogel catalyst. M.B. is grateful for financial support from the DFG.

Notes and references

1. S. Manandhar, P. B. Roder, J. L. Hanson, M. Lim, B. E. Smith, A. Mann and P. J. Pauzauskie, *J. Mater. Res.*, 2014, 29, 2905.
2. T. Yong-Jin Han, M. A. Worsley, T. F. Baumann and J. J. H. Satcher, *J. Mater. Chem.*, 2011, 21, 330.
3. R. Singh, R. K. Khardekar, D. K. Kohli, M. K. Singh, H. Srivastava and P. K. Gupta, *Mater. Lett.*, 2010, 64, 843.
4. J. Akl, T. Ghaddar, A. Ghanem and H. El-Rassy, *J. Mol. Catal. A: Chem.*, 2009, 312, 18.
5. O. Czakkel, E. Geissler, I. M. Szilágyi, E. Székely and K. László, *J. Colloid Interface Sci.*, 2009, 337, 513.
6. Y. Guo, W. Meyer-Zaika, M. Muhler, S. Vukojević and M. Epple, *Eur. J. Inorg. Chem.*, 2006, 2006, 4774.

7. C. Laberty-Robert, J. W. Long, E. M. Lucas, K. A. Pettigrew, R. M. Stroud, M. S. Doescher and D. R. Rolison, *Chem. Mater.*, 2006, 18, 50.
8. C. Moreno-Castilla and F. J. Maldonado-Hódar, *Carbon*, 2005, 43, 455.
9. H. Du, L. Gan, B. Li, P. Wu, Y. Qiu, F. Kang, R. Fu and Y. Zeng, *J. Phys. Chem. C*, 2007, 111, 2040.
10. B. C. Dunn, P. Cole, D. Covington, M. C. Webster, R. J. Pugmire, R. D. Ernst, E. M. Eyring, N. Shah and G. P. Huffman, *Appl. Catal., A*, 2005, 278, 233.
11. F. J. Maldonado-Hódar, C. Moreno-Castilla and A. F. Pérez-Cadenas, *Appl. Catal., B*, 2004, 54, 217.
12. K. Otsuka, K. Jinno and A. Morikawa, *J. Catal.*, 1986, 100, 353.
13. B. Neumann, T. W. Elkins, W. Dreher, H. Hagelin-Weaver, J. C. Nino and M. Baumer, *Catal. Sci. Technol.*, 2013, 3, 89.
14. L. Laitao, L. Songjun, D. Gengfeng and L. Fengyi, *React. Kinet. Catal. Lett.*, 2002, 75, 289.
15. R. B. Duarte, M. Nachtegaal, J. M. C. Bueno and J. A. van Bokhoven, *J. Catal.*, 2012, 296, 86.
16. J. Kärger and S. Vasenkov, *Microporous Mesoporous Mater.*, 2005, 85, 195.
17. J. Kärger, D. M. Ruthven and D. N. Theodorou, *Diffusion in Nanoporous Materials*, Wiley-VCH Verlag GmbH & Co. KGaA, Weinheim, Germany, 2012.
18. V. N. Burganos, *J. Chem. Phys.*, 1998, 109, 6772.
19. M. M. Tomadakis and S. V. Sotirchos, *AlChE J.*, 1993, 39, 397.
20. G. K. Papadopoulos, D. N. Theodorou, S. Vasenkov and J. Kärger, *J. Chem. Phys.*, 2007, 126, 094702/094701.
21. O. Geier, S. Vasenkov and J. Kärger, *J. Chem. Phys.*, 2002, 117, 1935.
22. M. Barrande, R. Bouchet and R. Denoyel, *Anal. Chem.*, 2007, 79, 9115.
23. Z. Sun, X. Tang and G. Cheng, *Microporous Mesoporous Mater.*, 2013, 173, 37.
24. R. Mueller, S. Zhang, B. Neumann, M. Bäumer and S. Vasenkov, *J. Chem. Phys.*, 2013, 139, 154703.
25. A. E. Gash, T. M. Tillotson, J. H. Satcher Jr, L. W. Hrubesh and R. L. Simpson, *J. Non-Cryst. Solids*, 2001, 285, 22.
26. A. E. Gash, J. H. Satcher Jr and R. L. Simpson, *J. Non-Cryst. Solids*, 2004, 350, 145.
27. S. J. Gibbs and C. S. Johnson Jr., *J. Magn. Reson.*, 1991, 93, 395.
28. S. Vasenkov, P. Galvosas, O. Geier, N. Nestle, F. Stallmach and J. Kärger, *J. Magn. Reson.*, 2001, 149, 228.
29. P. T. Callaghan, *Principles of NMR Microscopy*, Clarendon Press, Oxford, 1991.
30. M. Dvoyashkin, J. Zang, G. I. Yucelen, A. Katihar, S. Nair, D. S. Sholl, C. R. Bowers and S. Vasenkov, *J. Phys. Chem. C*, 2012, 116, 21350.
31. M. D. Mantle, D. I. Enache, E. Nowicka, S. P. Davies, J. K. Edwards, C. D'Agostino, D. P. Mascarenhas, L. Durham, M. Sankar, D. W. Knight, L. F. Gladden, S. H. Taylor and G. J. Hutchings, *J. Phys. Chem. C*, 2010, 115, 1073.
32. C. D'Agostino, J. Mitchell, L. F. Gladden and M. D. Mantle, *J. Phys. Chem. C*, 2012, 116, 8975.
33. R. Mueller, S. Zhang, C. Zhang, R. Lively and S. Vasenkov, J. Membr. Sci., 2015, 477, 123.
34. M. Cabrejas Manchado, J. M. Guil, A. Perez Masia, A. Ruiz Paniego and J. M. Trejo Menayo, *Langmuir*, 1994, 10, 685.
35. J. Baltrusaitis, J. H. Jensen and V. H. Grassian, *J. Phys. Chem. B*, 2006, 110, 12005.
36. D. Weber, A. J. Sederman, M. D. Mantle, J. Mitchell and L. F. Gladden, *PCCP*, 2010, 12, 2619.
37. S. P. Rigby, *Colloids Surf., A*, 2005, 262, 139.